CERN-INTC-2023-044 / INTC-P-667
19/04/2023

EUROPEAN ORGANIZATION FOR NUCLEAR RESEARCH

Proposal to the ISOLDE and Neutron Time-of-Flight Committee

High-resolution laser spectroscopy of light gold isotopes: investigation of "island of deformation" and shape coexistence

April 19, 2023

X. F. Yang,[1] S. W. Bai,[1] G. Neyens,[2] A. N. Andreyev,[3] M. Athanasakis-Kaklamanakis,[2,4] Y. Balasmeh,[2] S. Bara,[2] T. E. Cocolios,[2] J. G. Cubiss,[3] J. Dobaczewski,[3] R. P. de Groote,[2] K. T. Flanagan,[5] S. Franchoo,[6] R. F. Garcia Ruiz,[7] D. Hanstorp,[8] M. Heines,[2] H. R. Hu,[1] J. D. Johnson,[2] Á. Koszorús,[2,9] L. Lalanne,[4] Y. C. Liu,[1] Y. S. Liu,[1] K. M. Lynch,[5] A. McGlone,[5] M. Nichols,[8] F. Pastrana, [7] C. Page,[3] H. Perrett,[5] J. R. Reilly,[5] J. Trujillo,[2] P. Van Duppen,[2] S. G. Wilkins,[7] Z. X. Yue,[3]

[1]*School of Physics and State Key Laboratory of Nuclear Physics and Technology, Peking University, Beijing 100871, China*

[2]*KU Leuven, Instituut voor Kern- en Stralingsfysica, B-3001 Leuven, Belgium*

[3]*School of Physics, Engineering and Technology,University of York, Heslington, York, YO10 5DD, UK*

[4]*Experimental Physics Department, CERN, CH-1211 Geneva 23, Switzerland*

[5]*School of Physics and Astronomy, The University of Manchester, Manchester M13 9PL, United Kingdom*

[6]*Institut de Physique Nucléaire Orsay, IN2P3/CNRS, 91405 Orsay Cedex, France*

[7]*Massachusetts Institute of Technology, Cambridge, MA 02139, USA*

[8]*Department of Physics, University of Gothenburg, SE-412 96 Gothenburg, Sweden*

[9]*Belgian Nuclear Research Centre (SCK CEN), Boeretang 200, 2400, Mol, Belgium*

Spokesperson: X. F. Yang [xiaofei.yang@pku.edu.cn]
Co-Spokesperson: S. W. Bai [baisw@pku.edu.cn]
G. Neyens [gerda.neyens@kuleuven.be]
Contact person: L. Lalanne [louis-alexandre.lalanne@cern.ch]

Abstract: We propose to measure the ground- and isomeric- state properties of gold ($Z = 79$) isotopes around neutron mid-shell at $N = 104$ using the Collinear Resonance Ionization Spectroscopy (CRIS) setup. With this, we can extract nuclear properties, in particular spins and quadrupole moments, from the high-resolution hyperfine structure spectra. Our results will provide detailed information on the "island of deformation" characterized by the large nuclear radii observed in the light gold isotopes. Crucially, the quadrupole moments will provide information on the deformation of the ground- and long-lived excited states, and new insight on shape coexistence in this region.

Requested shifts: 19 shifts in one run.

1 Introduction

The region of neutron-deficient nuclei around $Z = 82$ and in the vicinity of the neutron mid-shell at $N = 104$ has been the subject of sustained experimental and theoretical interest. This effort was initiated with the observation of the large shape staggering in the nuclear charge radii of the neutron-deficient mercury isotopes ($Z = 80$) five decades ago [1, 2, 3]. Recent charge radii studies on lighter $^{177-180}$Hg isotopes revealed nearly spherical shapes and confirmed the absence of shape staggering for the lightest nuclei [4], as shown in Fig. 1 (a). The large shape staggering phenomenon in light mercury isotopes was interpreted by Monte Carlo Shell Model (MCSM) calculations as being due to proton excitations to the intruder $\pi 1h_{9/2}$ orbit leading to enhanced neutron occupation in the $\nu 1i_{13/2}$ orbit [4, 5]. This results in large quadrupole deformation of the neutron-odd ^{181,183,185}Hg isotopes in the $N = 104$ mid-shell region. Another example of large shape staggering was recently observed in the neutron-deficient bismuth isotopes ($Z = 83$), which starts at the exact same neutron number ($N = 105$) as mercury [6] and possesses a similar magnitude (Fig. 1(a)). In contrast, the charge radii of the neutron-deficient semi-magic lead ($Z = 82$) isotopes (Fig. 1(a)) indicate that these nuclei remain spherical down to $N = 101$ [7]. A sudden onset of strong deformation was also observed through measurements of the charge radii of the neighbouring gold ($Z = 79$) isotopes (Fig. 1(a)), where the deformation starts earlier in neutron number ($N = 107$) with respect to the closed shell at $N = 126$ [8] and remains constantly large down to $N = 101$, as demonstrated recently by an in-source resonance-ionization spectroscopy (RILIS) experiment [9, 10, 11]. The corresponding deformation parameter, $\langle\beta_2^2\rangle^{1/2}$, which is estimated from the droplet model [10, 12] and contributed by both static and dynamic deformation, lies around 0.25 and 0.30, reflecting a characteristic "island of deformation". Below $N = 101$ the isotopes return to sphericity, but a remarkable shape change was observed locally in ^{178}Au at $N = 99$, both for the ground state and the long-lived isomeric state. However, firm spin assignments were challenging with the low-resolution hyperfine structure (hfs) spectra obtained from RILIS experiment, therefore no firm conclusion on the magnetic moments of ^{178g,m}Au could be made and the underlying mechanism for the onset of deformation has not yet been fully established [13].

As most of the gold isotopes were studied by RILIS and the achieved spectral resolution limits measurement of the quadrupole moments, only magnetic moments and charge radii could be extracted from the measured hfs spectra. The information on the quadrupole moments of $^{177-188}$Au around neutron mid-shell at $N = 104$ remains very scarce, as shown in Tab. 1 and Fig. 1(b). In this proposal, we plan to measure the quadrupole moments and the spins of multiple states in $^{177-188}$Au using high-resolution collinear resonance ionization spectroscopy (CRIS). This new experimental information will provide the missing piece of information for establishing the electromagnetic properties of these states, which are essential for interpreting the phenomena in the region. We will also reveal the structure of the two long-lived states in ^{178}Au, by measuring their spins, magnetic moments and quadrupole moments. This will lead to a better understanding of the underlying mechanisms leading to the "island of deformation" and shape coexistence.

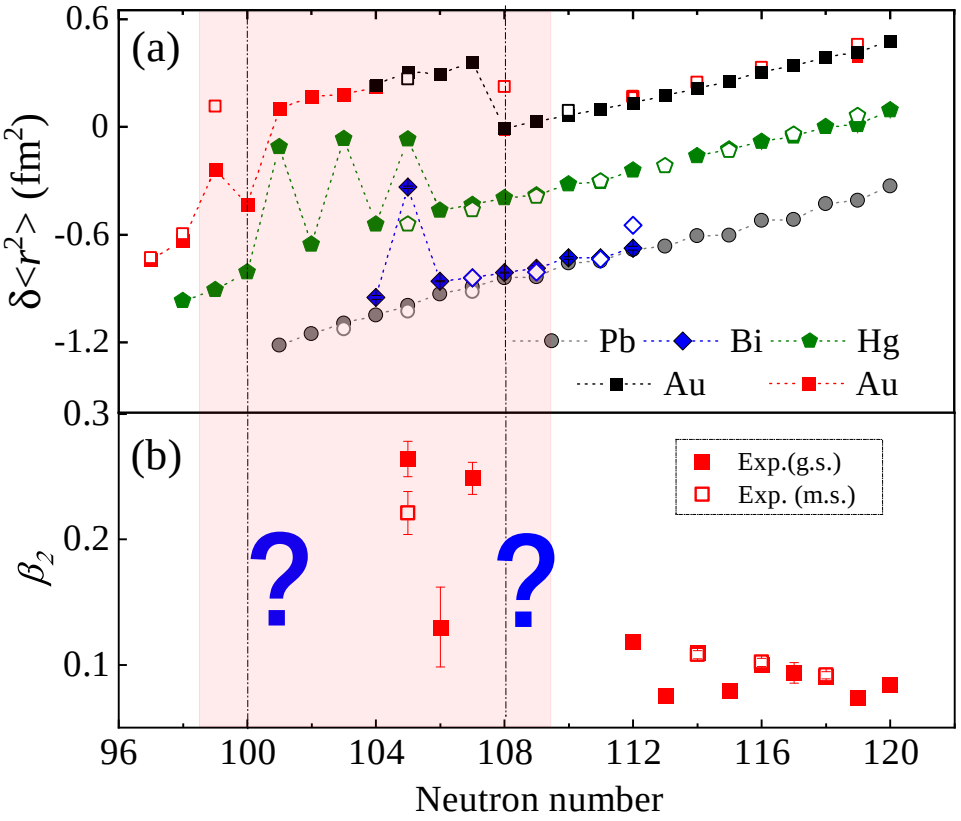

Figure 1: (a) Changes in mean square charge radii of several isotopic chains in lead region, which are arbitrarily offset for better visualization. Data are taken from Ref. [7] for lead, Ref. [6] for Bi, Ref. [4] for Hg and Ref. [8] for Au. The red squares for gold isotopes present recent unpublished results measured using RILIS [9, 10, 11]. (b) Deformation parameter β_2 evaluated from experimental quadrupole moments of gold isotopes (Table 1) and assuming weak coupling with $K = I$.

2 Physics Motivations

Nuclear quadrupole moments are sensitive to nuclear shapes, which could provide the information on the static deformation of the atomic nuclei. Thus, this observable is a sensitive probe of the "island of deformation" in the light gold isotopes which is established mostly by the nuclear charge radii. Figure 1 (b) shows the quadrupole deformation parameters (β_2) deduced from the available experimental quadrupole moments of gold isotopes (Tab. 1). Even with the very limited experimental data points, we see a clear correlation in the onset of deformation, between the β_2 deduced from Q_s and the trend in nuclear charge radii. We will further study the transitions from spherical to weakly- and strongly-deformed states, by measuring the quadrupole moments of the ground and isomeric states of $^{177-188}$Au isotopes covering the full region of "island of deformation". Although from the general trend of charge radii in Fig. 1 (a), the "island of deformation" in gold isotopes seems to end at $N = 101$, the sudden increase of the nuclear size in both ground and isomeric states of ^{178}Au ($N = 99$) raises question about the evolution of nuclear structure. Thus, measuring the quadrupole moments of isotopes around the ^{178}Au, in particular ^{177m}Au, is key to investigating this shape transitional region in the most neutron-deficient gold isotopes. In addition, the nuclear spins of many gold isotopes and isomers are so far only tentatively assigned, as summarized in Tab. 1. **Our**

Table 1: Summary of the available experimental electromagnetic moments for the ground and isomeric states of the gold isotopes. Those marked with red ✓ are measured but not yet published, while marker ? indicates these states have been measured, but data are not conclusive due to the unknown spins.

Isotope	Half-life	Spin	μ (μ_N)	Q_s (b)	$\delta\langle r^2\rangle$	Refs.
$^{177}Au_{98}$	1.53 s	$1/2^+$	1.15(5)		✓	[16, 10]
$^{177m}Au_{98}$	1 s	$(11/2^-)$	6.348(6)	-	✓	[17, 10]
$^{178}Au_{99}$	3.4 s	(2,3)	?	-	✓	[10, 13]
$^{178m}Au_{99}$	2.7 s	(7,8)	?	-	✓	[10, 13]
$^{179}Au_{100}$	7.1 s	$1/2^+$	1.01(5)		✓	[16, 10]
$^{180}Au_{101}$	8.4 s	(1^+)	-0.83(9)	-	✓	[18, 10]
$^{181}Au_{101}$	13.7 s	$(3/2^-)$	?	-	✓	[10]
$^{182}Au_{103}$	15.5 s	(2^+)	1.66(9)	-	✓	[18, 10]
$^{183}Au_{104}$	42.8 s	$(5/2^-)$	1.972(23)	-	✓	[19, 20]
$^{184}Au_{105}$	20.6 s	5^+	2.07(2)	4.65(26)	✓	[19, 21]
$^{184m}Au_{105}$	47.6 s	2^+	1.44(2)	1.90(16)	✓	[21]
$^{185}Au_{106}$	4.25 m	$5/2^-$	2.193(61)	-1.10(10)	✓	[17, 22, 23, 24]
$^{186}Au_{107}$	10.7 m	3^-	–1.202(60)	3.10(6)	✓	[17, 22, 23, 24]
$^{187}Au_{108}$	8.2 m	$1/2^+$	0.557(41)		✓	[17, 25, 22, 23]
$^{187m}Au_{108}$	2.3 s	$9/2^-$	3.529(53)	-	✓	[26]
$^{188}Au_{109}$	8.84 m	1^-	-0.07(3)	-	✓	[22, 23]

proposed CRIS experiment allows unambiguous measurement of the nuclear spins, which together with the magnetic moments and measured quadrupole moments (for states with $I > 1/2$) will provide all observables to probe the configuration of these nuclear states in detail. The quadrupole moments combining the charge radii will provide important information on the nature of the deformation and the degree to which these nuclei are statically deformed. Additionally, these observables can be compared to the theoretical calculations using different approaches available in this mass region, such as the MCSM [4, 5], Hartree-Fock-Bogoliubov (HFB) calculations [11, 14, 6], and Density Functional Theory (DFT) [15].

The phenomenon of shape coexistence has been widely studied by means of large isomer shifts between intruder and normal states in several isotopic chains of this region [27], for example in mercury [28], thallium [29], bismuth [30]. A large number of isomeric states have been identified in gold isotopes, as summarized in Tab. 1, and large isomer shifts have been observed in ^{178,187}Au isotopes, as seen in Fig. 1(a). Thus, the proposed measurements of quadrupole moments will be useful for the study of the possible shape coexistence in these two isotopes. For ^{187}Au, the magnetic moments of its $9/2^-$ isomer and $1/2^+$ ground state were also measured [26]. The $9/2^-$ isomer is explained in Ref. [26] as a member of a rotational band built upon the $1/2^-[541]$ Nilsson orbit at prolate deformation based on the Particle Triaxial Rotor Model (PTRM) calculation [16, 26], which is different from that in thallium where the $9/2^-$ state is based on the $9/2[505]$ Nilsson orbit at moderate

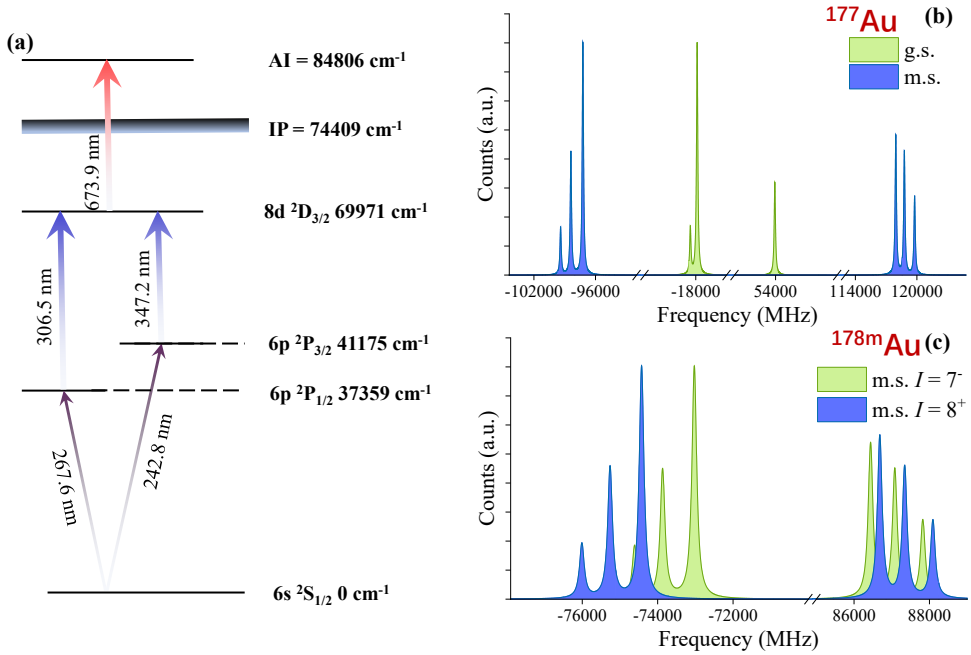

Figure 2: (a) Resonance ionization schemes for gold [21, 31, 16]. The first step of $^2S_{1/2} \rightarrow {}^2P_{3/2}$ is proposed for the quadrupole moment measurements of gold isotopes in this proposal. (b-c) Simulated hfs spectra of $^2S_{1/2} \rightarrow {}^2P_{3/2}$ transition (including only the magnetic hyperfine interaction) for ^{177g,m,178m}Au assuming a linewidth of 150 MHz. As the spins for ^{178}Au have not been unambiguously determined, only the hfs spectrum for its isomeric state with different spin assumption (7^- and 8^-) is included.

oblate deformation. **Quadrupole moment measurement of the $9/2^-$ isomer in ^{187}Au will directly prove or disprove this interpretation, as the quadrupole moment will be a sensitive probe of its configuration.** For ^{178}Au, the spins of its ground and isomeric states could not be firmly assigned (Table 1) [13], and thus their magnetic moments (dependent on the spin assignment) could only suggest the most probable configurations for these two states [13]. **The proposed high-resolution laser spectroscopy measurement of ^{178g,m}Au will allow measurement of their spins, and the magnetic and quadrupole moments, which will offer information on the configurations and shapes of these states and thus investigate the phenomenon of shape coexistence.**

3 High-resolution CRIS experiment

In order to extract the nuclear properties, in particular the spins and quadrupole moments, the CRIS setup [32] will be used to measure the high-resolution hfs spectra of ground and isomeric states of gold isotopes. While hfs spectrum of $^2S_{1/2} \rightarrow {}^2P_{1/2}$ transition with RILIS was measured with a resolution of about 5 GHz [18], at CRIS we can achieve a higher resolution of about 150 MHz estimated conservatively [33, 34]. This enables us to probe the $^2S_{1/2} \rightarrow {}^2P_{3/2}$ transition (Fig. 2(a)), and thus allow measurement of spins and quadrupole moments from the hfs spectra [27] as simulated in Fig. 2(c).

The gold isotopes will be produced at ISOLDE by impinging the 1.4 GeV protons on a

thick UC_x target. The produced gold atoms will be selectively ionized by the Resonance Ionization Laser Ion Source (RILIS), extracted and then mass separated by the High Resolution Separator (HRS) [35, 31]. After being cooled and bunched in a linear Paul trap [36], the bunched ions will be delivered into the CRIS setup where they are first neutralized in a charge exchange cell (CEC) filled with Na vapour. It is worth noting that the $^2S_{1/2}$ state is highly populated ($> 65\%$) in this process [37]. A deflector and a field ionization electrode mounted downstream of the CEC eliminates the remaining ions or atoms in highly excited states [32]. The gold atoms will then be sent to the interaction region (IR) to be overlapped in space and time with several pulsed laser beams. The IR is maintained at ultra-high vacuum ($\sim 10^{-10}$ mbar) in order to suppress non-resonant collisional ionization. The resonantly ionized ions will subsequently be deflected into the ion detection chamber where a MagneTOF ion detector will be used to count the ions. The hfs spectrum is reconstructed by counting ions as a function of the laser frequency detuning.

Figure 2(a) presents the three-step laser ionization schemes for the gold atom, which have been extensively studied previously [21, 31, 16]. The transition of $^2S_{1/2} \rightarrow {}^2P_{1/2}$ (267.6 nm), which is not sensitive to the quadrupole interaction, has often been used for the measurement of nuclear magnetic moments [38, 16, 17, 26]. For the measurement of quadrupole moments, the $^2S_{1/2} \rightarrow {}^2P_{3/2}$ (242.8 nm) transition will be used [21] as the hfs $B_{^{197}\mathrm{Au}} = 336(10)$ MHz parameter of $^2P_{3/2}$ [21] is sufficiently sensitive to the quadrupole moment. Thus, the proposed ionization scheme for the quadrupole moment measurements of gold isotopes in this work is 242.8 nm + 347.2 nm + 673.9 nm. The frequency-tripled injection-locked Ti:Sapphire laser (bandwidth of $\sim$20 MHz before tripling) in the CRIS laser lab will be used for the first scanning step, enabling a linewidth of about 150 MHz [33, 34]. The second and third steps can be provided with the existing doubled pulsed dye laser and fundamental dye laser, respectively.

4 Production yields and beam time request

As summarized in Fig. 3 and Tab. 2, the production yields of $^{177-188}$Au isotopes (blue squares) have been reported recently at ISOLDE [39], together with the in-target production (red curve) calculated by the FLUKA-CERN code. As noted in Ref. [39], the reported yields were measured in the narrow-band mode of the RILIS, which are expected to be increased by a factor of 2–3 when using RILIS in broad-band mode (blue shadow curve in Fig. 3).

The requested shifts for the CRIS measurements of $^{177-188}$Au isotopes are summarized in Tab. 2, which are estimated based on the efficiency of the CRIS by using three-step

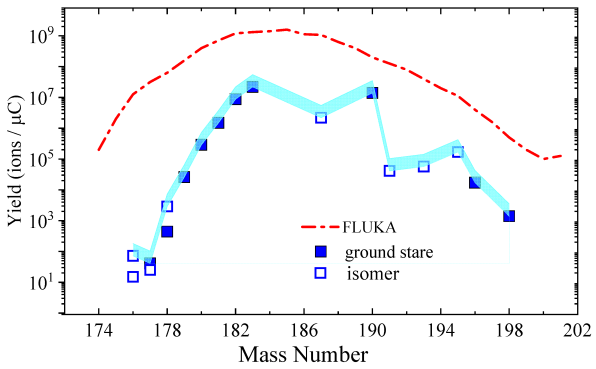

Figure 3: Measured (blue dots) and calculated in-target production (red curve) yields for gold isotopes at ISOLDE [39]. Blue shadow curve presents the enhancement in production yield by using RILIS in broad-band mode [39].

Table 2: Summary of yields of gold isotopes at ISOLDE [39] and shifts requested. As noted in Ref [39], the reported yields can be increased by a factor of 2–3 when using RILIS in broad-band mode.

A	$T_{1/2}$	Nr. of States	Yield (ions/μC)	RILIS [39] (ions/μC)	Shifts
$177(g,m)$	1.5 s / 1.19 s	2	41 / 25	102/63	6
$178(g,m)$	3.4 s / 2.7 s	2	4.4×10^2 / 2.9×10^3	$\sim 10^3$	4
$179-188(g,m)$		12	$> 2\times10^4$	$> 10^4$	6
Reference scans for hfs measurements					3
Total:					**19**
Stable beam (^{197}Au) for optimization of the experimental setup					2

laser ionization, the scanning range of the hfs spectra of gold isotopes as well as the production yields [40, 41].

For isotopes with a yield above 10^4 ions/s, e.g.$^{179-188}$Au, the data taking time is mostly determined by the frequency range of the hfs spectra, which is several GHz for one state in the case of gold isotopes (Fig. 2(b-c)). For each nuclear state of the gold isotopes, the estimated frequency range for the hfs spectra of $^2S_{1/2} \rightarrow {}^2P_{3/2}$ transition is about 6-8 GHz (Fig. 2(b-c)). Thus, we request 0.5 shift to scan the hfs spectra for each state of the isotopes. In total, 6 shifts are requested to measure the 12 nuclear states of $^{179-188}$Au. For the isotopes with a yield below 10^4 ions/s, the number of shifts can be estimated based on the earlier study at CRIS [33, 42]. For the measurement of ^{78}Cu with a yield of 20 ions/s [33, 42], one shift was sufficient to scan a frequency range of 2 GHz and to obtain a hfs spectrum with sufficient statistics. Therefore, for the most exotic case of ^{177g,m}Au with a production yield below $\sim$100 ions/s, 6 shifts are requested to scan the estimated frequency range of about 7 GHz (Fig. 2(b)) for both ground and isomeric states. For the largely deformed ground and isomeric states of ^{178}Au, which has a production yield of 10^3 ions/s and 10^2 ions/s, respectively, we request 4 shifts to scan the estimated frequency range of about 7 GHz (Fig. 2(c)) for both ground and isomeric states. Therefore, in total, 16 shifts are requested to measure the quadrupole moments, magnetic moments and spins of $^{177-188}$Au isotopes. In order to monitor the stability of the experimental conditions and also extract charge radii from our data, reference measurements need to be performed at regular time intervals on one specific isotope. This would require an additional 3 shifts. Note that an experiment to measure the masses of neutron-rich gold isotopes ($A > 199$) has already been proposed [43], which motivates a future high-resolution laser spectroscopy experiment to be planned to study the neutron-rich isotopes.

Summary of requested shifts: 19 shifts are requested using a UC$_x$ target. In addition, 2 shifts of stable beam are requested for optimization.

References

[1] J. Bonn, G. Huber, H.-J. Kluge, L. Kugler, and E.W. Otten. Sudden change in the nuclear charge distribution of very light mercury isotopes. *Physics Letters B*, 38(5):308–311, 1972.

[2] J. Bonn, G. Huber, H. J. Kluge, et al. Spins, moments and charge radii in the isotopic series ^{181}Hg-^{191}Hg. *Zeitschrift für Physik A Atoms and Nuclei*, 276:203–217, Sep 1976.

[3] T. Kühl, P. Dabkiewicz, C. Duke, H. Fischer, H. J. Kluge, H. Kremmling, and E. W. Otten. Nuclear shape staggering in very neutron-deficient Hg isotopes detected by laser spectroscopy. *Phys. Rev. Lett.*, 39:180–183, Jul 1977.

[4] B. A. Marsh, T. Day Goodacre, S. Sels, et al. Characterization of the shape-staggering effect in mercury nuclei. *Nature Physics*, 14:1163–1167, Dec 2018.

[5] S. Sels, T. Day Goodacre, B. A. Marsh, et al. Shape staggering of midshell mercury isotopes from in-source laser spectroscopy compared with density-functional-theory and monte carlo shell-model calculations. *Phys. Rev. C*, 99:044306, Apr 2019.

[6] A. Barzakh, A. N. Andreyev, C. Raison, et al. Large shape staggering in neutron-deficient bi isotopes. *Phys. Rev. Lett.*, 127:192501, Nov 2021.

[7] H. De Witte, A. N. Andreyev, N. Barré, et al. Nuclear charge radii of neutron-deficient lead isotopes beyond $N = 104$ midshell investigated by in-source laser spectroscopy. *Phys. Rev. Lett.*, 98:112502, Mar 2007.

[8] K. Wallmeroth, G. Bollen, A. Dohn, et al. Nuclear shape transition in light gold isotopes. *Nuclear Physics A*, 493(2):224–252, 1989.

[9] Andrei Andreyev and Anatoly Barzakh. Part I: β-delayed fission, laser spectroscopy and shape-coexistence studies with astatine beams; Part II: Delineating the island of deformation in the light gold isotopes by means of laser spectroscopy. *CERN-INTC-2013-002, INTC-P-319-ADD-1*, 2013.

[10] B. Andel, A. N. Andreyev, S. Antalic, et al. Laser assisted studies of β-delayed fission in ^{178,176}Au and of the structure of ^{175}Au. *CERN-INTC-2020-032, INTC-P-558*, 2020.

[11] J. Cubiss, A. N. Andreyev, et al. *submitted (Private communication)*, 2023.

[12] William D. Myers and Karl-Heinz Schmidt. An update on droplet-model charge distributions. *Nuclear Physics A*, 410(1), 1983.

[13] J. G. Cubiss, A. N. Andreyev, A. E. Barzakh, et al. Laser-assisted decay spectroscopy and mass spectrometry of ^{178}Au. *Phys. Rev. C*, 102:044332, Oct 2020.

[14] V. Manea, P. Ascher, D. Atanasov, A. E. Barzakh, D. Beck, K. Blaum, Ch. Borgmann, M. Breitenfeldt, R. B. Cakirli, T. E. Cocolios, T. Day Goodacre, D. V. Fedorov, V. N. Fedosseev, S. George, F. Herfurth, M. Kowalska, S. Kreim, Yu. A. Litvinov, D. Lunney, B. Marsh, D. Neidherr, M. Rosenbusch, R. E. Rossel, S. Rothe, L. Schweikhard, F. Wienholtz, R. N. Wolf, and K. Zuber. Penning-trap mass spectrometry and mean-field study of nuclear shape coexistence in the neutron-deficient lead region. *Phys. Rev. C*, 95:054322, May 2017.

[15] J. Bonnard, J. Dobaczewski, G. Danneaux, and M. Kortelainen. Nuclear DFT electromagnetic moments of intruder configurations calculated in heavy deformed open-shell odd nuclei with $63 \leq Z \leq 82$ and $82 \leq N \leq 126$. *arXiv:2209.09156*, Sep 2022.

[16] J.G. Cubiss, A.E. Barzakh, A.N. Andreyev, et al. Change in structure between the $I = 1/2$ states in ^{181}Tl and ^{177,179}Au. *Physics Letters B*, 786:355–363, 2018.

[17] A. E. Barzakh, D. Atanasov, A. N. Andreyev, et al. Hyperfine anomaly in gold and magnetic moments of $I^{\pi} = 11/2^{-}$ gold isomers. *Phys. Rev. C*, 101:034308, Mar 2020.

[18] R. D. Harding, A. N. Andreyev, A. E. Barzakh, et al. Laser-assisted decay spectroscopy for the ground states of ^{180,182}Au. *Phys. Rev. C*, 102:024312, Aug 2020.

[19] U. Krönert, St. Becker, G. Bollen, et al. On-line laser spectroscopy by resonance ionization of laser-desorbed, refractory elements. *Nuclear Instruments and Methods in Physics Research Section A: Accelerators, Spectrometers, Detectors and Associated Equipment*, 300(3):522–537, 1991.

[20] U. Krönert, St. Becker, G. Bollen, et al. Observation of strongly deformed ground-state configurations in ^{184}Au and ^{183}Au by laser spectroscopy. *Zeitschrift für Physik A Atomic Nuclei*, 331:521–522, 1988.

[21] F. Le Blanc, J. Obert, J. Oms, et al. Nuclear moments and deformation change in ^{184}Au^{g,m} from laser spectroscopy. *Phys. Rev. Lett.*, 79:2213–2216, Sep 1997.

[22] K. Wallmeroth, G. Bollen, M. J. G. Borge, et al. Nuclear shape transition in neutron-deficient gold isotopes. *Hyperfine Interactions*, 34:21–24, Mar 1987.

[23] K. Wallmeroth, G. Bollen, A. Dohn, et al. Sudden change in the nuclear charge distribution of very light gold isotopes. *Phys. Rev. Lett.*, 58:1516–1519, Apr 1987.

[24] N.J. Stone. Table of nuclear electric quadrupole moments. *INDC International Nuclear Data Committee*, Oct 2021.

[25] G. Savard, J.E. Crawford, J.K.P. Lee, et al. Laser spectroscopy of laser-desorbed gold isotopes. *Nuclear Physics A*, 512(2):241–252, 1990.

[26] A. E. Barzakh, D. Atanasov, A. N. Andreyev, et al. Shape coexistence in ^{187}Au studied by laser spectroscopy. *Phys. Rev. C*, 101:064321, Jun 2020.

[27] X.F. Yang, S.J. Wang, S.G. Wilkins, and R.F. Garcia Ruiz. Laser spectroscopy for the study of exotic nuclei. *Progress in Particle and Nuclear Physics*, page 104005, 2022.

[28] P. Dabkiewicz, F. Buchinger, H. Fischer, H.-J. Kluge, H. Kremmling, T. Khl, A.C. Mller, and H.A. Schuessler. Nuclear shape isomerism in ^{185}Hg detected by laser spectroscopy. *Physics Letters B*, 82(2):199–203, 1979.

[29] A. E. Barzakh, A. N. Andreyev, T. E. Cocolios, R. P. de Groote, D. V. Fedorov, V. N. Fedosseev, R. Ferrer, D. A. Fink, L. Ghys, M. Huyse, U. Köster, J. Lane, V. Liberati, K. M. Lynch, B. A. Marsh, P. L. Molkanov, T. J. Procter, E. Rapisarda, S. Rothe, K. Sandhu, M. D. Seliverstov, A. M. Sjödin, C. Van Beveren, P. Van Duppen, M. Venhart, and M. Veselský. Changes in mean-squared charge radii and magnetic moments of $^{179--184}$Tl measured by in-source laser spectroscopy. *Phys. Rev. C*, 95:014324, Jan 2017.

[30] A. E. Barzakh, D. V. Fedorov, V. S. Ivanov, P. L. Molkanov, F. V. Moroz, S. Yu. Orlov, V. N. Panteleev, M. D. Seliverstov, and Yu. M. Volkov. Laser spectroscopy studies of intruder states in ^{193,195,197}Bi. *Phys. Rev. C*, 94:024334, Aug 2016.

[31] B. A. Marsh, V. N. Fedosseev, P. Kosuri, et al. Development of a RILIS ionisation scheme for gold at ISOLDE, CERN. *Hyperfine Interactions*, 171:109–116, 2006.

[32] A.R. Vernon, R.P. de Groote, J. Billowes, et al. Optimising the collinear resonance ionisation spectroscopy (CRIS) experiment at CERN − ISOLDE. *Nuclear Instruments and Methods in Physics Research Section B: Beam Interactions with Materials and Atoms*, 463:384–389, 2020.

[33] R. P. de Groote et al. Dipole and quadrupole moments of $^{73-78}$Cu as a test of the robustness of the $Z = 28$ shell closure near ^{78}Ni. *Physical Review C*, 96:041302(R), 2017.

[34] A. R. Vernon, R. F. Garcia Ruiz, T. Miyagi, et al. Nuclear moments of indium isotopes reveal abrupt change at magic number 82. *Nature*, 607:260–265, 2022.

[35] Valentin Fedosseev, Katerina Chrysalidis, Thomas Day Goodacre, et al. Ion beam production and study of radioactive isotopes with the laser ion source at ISOLDE*. *Journal of Physics G: Nuclear and Particle Physics*, 44(8):084006, Jul 2017.

[36] E. Mané, J. Billowes, S. Antalic, et al. An ion cooler-buncher for high-sensitivity collinear laser spectroscopy at isolde. *The European Physical Journal A*, 42:503–507, Dec 2009.

[37] A.R. Vernon, J. Billowes, C.L. Binnersley, et al. Simulation of the relative atomic populations of elements $1 \leq Z \leq 89$ following charge exchange tested with collinear resonance ionization spectroscopy of indium. *Spectrochimica Acta Part B: Atomic Spectroscopy*, 153:61–83, 2019.

[38] R. D. Harding, A. N. Andreyev, A. E. Barzakh, et al. Laser-assisted nuclear decay spectroscopy of ^{176,177,179}Au. *Phys. Rev. C*, 104:024326, Aug 2021.

[39] A.E. Barzakh, A.N. Andreyev, D. Atanasov, et al. Producing gold at ISOLDE – CERN. *Nuclear Instruments and Methods in Physics Research Section B: Beam Interactions with Materials and Atoms*, 513:26–32, 2022.

[40] Xiaofei Yang. Study of neutron-rich ^{52,53}K isotopes by the measurement of spins, moments and charge radii. Technical report, CERN, Geneva, 2016.

[41] Xiaofei Yang, Thomas Cocolios, and Sarina Geldhof. Probing the magicity and shell evolution in the vicinity of $N = 50$ with high-resolution laser spectroscopy of ^{81,82}Zn isotopes. Technical report, CERN, Geneva, 2020.

[42] R. P. de Groote et al. Measurement and microscopic description of odd-even staggering of charge radii of exotic copper isotopes. *Nature Physics*, 16:620–624, 2020.

[43] Vladimir Manea, Klaus Blaum, Daniel Lange, et al. Exploring the evolution of the $N = 126$ magic number withthe masses of neutron-rich gold isotopes. *CERN-INTC-2023-005, INTC-P-650*, 2023.

Appendix

DESCRIPTION OF THE PROPOSED EXPERIMENT

The experimental setup comprises: (*name the fixed-ISOLDE installations, as well as flexible elements of the experiment*)

Part of the	Availability	Design and manufacturing
CRIS	☒ Existing	☒ To be used without any modification

HAZARDS GENERATED BY THE EXPERIMENT Hazards named in the document relevant for the fixed CRIS installation.